Cancer Research

Stearoyl-CoA Desaturase 1 Protects Ovarian Cancer Cells from Ferroptotic Cell Death

Lia Tesfay[1], Bibbin T. Paul[1], Anna Konstorum[2], Zhiyong Deng[1], Anderson O. Cox[3], Jingyun Lee[3], Cristina M. Furdui[3,4], Poornima Hegde[5], Frank M. Torti[6], and Suzy V. Torti[1]

Abstract

Activation of ferroptosis, a recently described mechanism of regulated cell death, dramatically inhibits growth of ovarian cancer cells. Given the importance of lipid metabolism in ferroptosis and the key role of lipids in ovarian cancer, we examined the contribution to ferroptosis of stearoyl-CoA desaturase (SCD1, *SCD*), an enzyme that catalyzes the rate-limiting step in monounsaturated fatty acid synthesis in ovarian cancer cells. SCD1 was highly expressed in ovarian cancer tissue, cell lines, and a genetic model of ovarian cancer stem cells. Inhibition of SCD1 induced lipid oxidation and cell death. Conversely, overexpression of *SCD* or exogenous administration of its C16:1 and C18:1 products, palmitoleic acid or oleate, protected cells from death. Inhibition of SCD1 induced both ferroptosis and apoptosis. Inhibition of SCD1 decreased CoQ_{10}, an endogenous membrane antioxidant whose depletion has been linked to ferroptosis, while concomitantly decreasing unsaturated fatty acyl chains in membrane phospholipids and increasing long-chain saturated ceramides, changes previously linked to apoptosis. Simultaneous triggering of two death pathways suggests SCD1 inhibition may be an effective component of antitumor therapy, because overcoming this dual mechanism of cell death may present a significant barrier to the emergence of drug resistance. Supporting this concept, we observed that inhibition of SCD1 significantly potentiated the antitumor effect of ferroptosis inducers in both ovarian cancer cell lines and a mouse orthotopic xenograft model. Our results suggest that the use of combined treatment with SCD1 inhibitors and ferroptosis inducers may provide a new therapeutic strategy for patients with ovarian cancer.

Significance: The combination of SCD1 inhibitors and ferroptosis inducers may provide a new therapeutic strategy for the treatment of ovarian cancer patients.

See related commentary by Carbone and Melino, p. 5149

Introduction

Ferroptosis is a recently described form of cell death that is distinct from other known cell death pathways (1). Interest in ferroptosis has been stimulated by its potential to be activated by anticancer drugs (1). Although the precise mechanism of ferroptotic cell death is not completely understood, lipid peroxidation has been identified as a critical mediator of ferroptosis. More specifically, elevated levels of phosphatidylethanolamine (PE) containing oxidized polyunsaturated fatty acyl chains (PUFA), particularly oxidized arachidonate (C20:4) and adrenate (C22:4), have been implicated in ferroptosis (2, 3).

Two key proteins limit the generation of lipid peroxides that induce ferroptosis. These are glutathione peroxidase 4 (GPX4), which reduces esterified oxidized fatty acids to their corresponding alcohols; and SLC7A11, a cystine antiporter that provides the cysteine needed for synthesis of glutathione, a cellular antioxidant and cofactor in the activity of GPX4 (1). Accordingly, small-molecule inhibitors of GPX4 or SLC7A11, such as RSL3 or erastin, respectively, induce ferroptosis (1). Other enzymes implicated in ferroptosis also center on lipid pathways, for example, inhibition of acyl-CoA synthetase long-chain family member 4 (ACSL4), which activates long-chain PUFAs for lipid synthesis, protects cells from ferroptosis (4), as does deletion of lysophosphatidylcholine acyltransferase 3 (LPCAT3), which is involved in the generation of PUFA-PEs (5). Conversely, inhibition of squalene synthase, which affects multiple metabolites in the mevalonate pathway including the lipophilic antioxidant CoQ_{10}, sensitizes cells to ferroptosis (6). Given the essential role of lipid peroxidation in ferroptosis, modulation of cellular lipid composition might be expected to perturb ferroptotic cell death.

Sterol CoA desaturase (SCD1, *SCD*) is a lipid-modifying enzyme that is upregulated in numerous malignancies, including prostate, liver, and breast cancers (7). SCD1 catalyzes the desaturation of saturated fatty acids, principally stearic acid (18:0) and palmitic acid (16:0), to their Δ9-monounsaturated counterparts, oleic acid (18:1) and palmitoleic acid (16:1; ref. 8). We considered that this enzyme might affect the sensitivity of cells to ferroptosis. In particular, we hypothesized that upregulation of SCD1 is an intrinsic cytoprotective mechanism that protects cancer cells from the cytotoxic action of ferroptosis inducers.

[1]Department of Molecular Biology and Biophysics, UConn Health, Farmington, Connecticut. [2]Center for Quantitative Medicine, UConn Health, Farmington, Connecticut. [3]Proteomics and Metabolomics Shared Resource, Comprehensive Cancer Center, Wake Forest University School of Medicine, Winston-Salem, North Carolina. [4]Department of Internal Medicine, Section on Molecular Medicine, Wake Forest University Health Sciences, Winston-Salem, North Carolina. [5]Department of Pathology, UConn Health, Farmington, Connecticut. [6]Department of Medicine, UConn Health, Farmington, Connecticut.

Note: Supplementary data for this article are available at Cancer Research Online (http://cancerres.aacrjournals.org/).

Corresponding Author: Suzy V. Torti, University of Connecticut Health Center, 263 Farmington Avenue, Farmington, CT 06030. Phone: 860-679-6503; Fax: 860-679-1255; E-mail: storti@uchc.edu

Cancer Res 2019;79:5355–66

doi: 10.1158/0008-5472.CAN-19-0369

To test this hypothesis, we focused on ovarian cancer and ovarian cancer stem cells, because our earlier work demonstrated that ovarian cancer stem cells are sensitive to the ferroptosis inducer erastin *in vitro* and *in vivo* (9). Cancer stem cells are believed to be a small, treatment-refractory subpopulation of tumor cells that seed metastases and give rise to treatment resistance. Thus, our experiments demonstrating sensitivity of cancer stem cells to ferroptosis, as well as results from other groups (10), suggest that there may be a role for ferroptosis inducers in the treatment of ovarian cancer. Further, recent work has shown that lipid desaturation is increased and contributes to the maintenance of stemness in ovarian cancer cells (11). Thus, ovarian cancer represents a particularly pertinent model in which to assess the role of SCD1 in the sensitivity to ferroptosis inducers.

Here, we demonstrate that SCD1, a lipid desaturase, alters lipid membrane composition and modulates ferroptosis. Further, inhibition of SCD1 enhances the antitumor effect of ferroptosis inducers in ovarian cancer both *in vitro* and *in vivo*.

Materials and Methods

Cell culture

MDAH2774, SW626, SKOV3, and TOV-112D cells were purchased from ATCC (on March 6, 2013). Cells were frozen at low passage and used within 2 to 3 months after thawing. Cells were cultured in DMEM (GIBCO) supplemented with 10% FBS (Gemini Bio-Products). COV362 cells were purchased from Sigma on May 18, 2015, and cultured in DMEM (GIBCO) containing 10% FBS. FT-t and FT-i cells (isolated by transfection of primary fallopian tube stem cells as described in ref. 12) were cultured in DMEM containing 10% FBS. Human ovarian surface epithelial (HOSE) cells (ScienCell Research Laboratories) were cultured in Ovarian Epithelial Cell Medium (ScienCell Research Laboratories). OVCAR-4 and OVCAR-8 cells were obtained from NCI (distributed by Charles River Labs) on February 25, 2018, and OVCAR5 cells were obtained on May 8, 2019. OVCAR-4, OVCAR-5, and OVCAR-8 cells were cultured in RPMI-1640 + L-glutamine (GIBCO) supplemented with 10% FBS (Gemini Bio-Products).

Infection and isolation of SCD1-expressing FT-t and COV362 cells

Human *SCD* cDNA was amplified using GE Dharmacon clone (cat. #MHS6278-202830110) and introduced into the lentiviral tetracycline (tet)-inducible vector pLVX-TetOne-Puro (Takara-Clontech) prior to infection of FT-t cells. For overexpression of *SCD* in COV362 cells *SCD* cDNA was amplified and inserted into the pLVX-TetOn-Puro vector. Lentivirus particles were produced by transient cotransfection of the SCD1 tet-on expression vector and packaging vectors (VSVG, pMDLG, and RSV-REV) into 293T cells. Viral particles containing control empty vector were prepared similarly. Cells were infected and selected for puromycin resistance for 2 weeks before experiments were performed.

shRNA knockdown of OVCAR4 cells

Knockdown of SCD1 In OVCAR4 cells was performed using a lentiviral shRNA vector (13) designed to target the sequence GCATTCCAGAATGATGTCTAT in the SCD1 coding region. Stable knockdown cells were isolated by selecting for puromycin resistance.

Quantitative real-time PCR

Quantitative real-time PCR (qRT-PCR) was performed as previously described (14) Primers used were human *SCD* forward: AAACCTGGCTTGCTGATG; human *SCD* reverse: GGGGGCTAATGTTCTTGTCA; human β-actin forward: TTG CCG ACA GGA TGC AGA AGG A; human β-actin reverse: AGG TGG ACA GCG AGG CCA GGA T.

Western blot

Western blotting was performed and quantified as previously described (9). Membranes were probed with antibodies to β-actin (Sigma; cat. #A3854) and SCD1 (Abcam; cat. #ab39969). HRP-conjugated goat anti-rabbit was used as a secondary antibody (Bio-Rad; cat. #170-5046).

Cell viability and cell death

Cells (2×10^3–3×10^3) were seeded in 96 well plates and treated with the following reagents: RSL3 (Selleckchem), erastin (Selleckchem), ferrostatin-1 (Selleckchem), MF-438 (Sigma), CAY10566 (Cayman), A939572 (Cayman), fatty acids [oleic acid, palmitoleic acid, stearic acid, or palmitic acid (Sigma)], zVAD-fmk (Selleckchem). Cell viability was assessed 24 to 72 hours post-treatment using calcein-AM (Millipore). FACS analysis of propidium iodide-stained cells was used to directly measure cell death (15).

Synergy

Synergism was computed using the Chou–Talalay method (16) with CalcuSyn software.

Caspase-3/7 activity

Cells (10,000) were treated with MF-438 in the presence or absence of zVAD-fmk (Selleckchem) for 48 hours or staurosporine (Sigma) for 4 hours. Caspase-3/7 activity was analyzed using Caspase-Glo 3/7 Assay Systems from Promega.

siRNA knockdown experiments

All reagents were obtained from GE Dharmacon. Twelve nanograms of ON-TARGETplus Human SCD1 siRNA (L-005061-00-0010) and siNTC (cat. #D-001810-10-05) were used for knockdown experiments. Transfections were performed according to the manufacturer's recommendations using Dharmafect #1 transfection reagent (cat. #T-2001). Knockdown efficiencies were confirmed at the time of harvest by qRT-PCR and/or by Western blotting.

IHC

Formalin-fixed paraffin-embedded slides of deidentified human tissues from high-grade serous ovarian cancer (HGSOC; 9 subjects) and normal ovary (6 subjects) were obtained from the biorepository of UConn Health (IRB IE-08-310-1). Tissues were immunostained with antibodies to human SCD1, followed by anti-rabbit secondary antibody (Biocare Medical MACH2 Rabbit HRP-Polymer; cat. #RHRP520), staining with 3,3′-diaminobenzidine (Biocare Medical) and counterstaining with Gill's Hematoxylin III and Lithium Blue (Poly Scientific). Competition with specific peptide (Abcam; #ab40137) was used as a control. Staining was quantified as described (see Supplementary Materials and Methods; ref. 17).

C11-BODIPY staining

Cells were plated in 8-chamber slides (BD Falcon) and treated with 1 to 5 μmol/L RSL3 in the presence or absence 2 μmol/L ferrostatin-1 (Fer-1) for 4 hours prior to incubation with 2 μmol/L C11-BODIPY (Thermo Fisher Scientific) for 30 minutes. Slides were washed, fixed with 4% paraformaldehyde (Thermo Fisher Scientific), and mounted using ProLong Gold anti-fade reagent (Invitrogen). Images were acquired using inverted microscopy (Zeiss Axio Vert.A1). For flow cytometry, cells were washed subsequent to staining with C11-bodipy analyzed using a BD LSRII flow cytometer (Becton Dickinson).

Animal experiments

Female NOD.Cg-Prkdcscid Il2rgtm1Wjl/SzJ mice (NSG; ~6 weeks of age) were obtained from The Jackson Laboratory. FT-t cells (100,000) were injected intraperitoneally (i.p.; $n = 8$/group). The next day, mice were injected i.p. with 1 mg/kg A939572 in corn oil (Sigma) in the presence or absence of 20 mg/kg erastin in 2% DMSO (Thermo Fisher Scientific) in corn oil. Vehicle (2% DMSO in corn oil) was used as a control. Treatment was continued at 5 doses per week for 18 days, when control mice began to develop ascites and become moribund. Mice were sacrificed, tumors were counted, and the combined weight of all tumors within the abdomen of each mouse was measured. Histologic evaluation of representative nodules by a board-certified pathologist (P. Hegde) confirmed that they were high-grade tumors with multiple mitotic figures and areas of necrosis. Group size was based on power calculations and was designed to provide 80% power to detect an effect size of 0.5 g difference in tumor mass using two-sided *t* tests. Two animals in the A939572 group and the combined treatment group died for unknown reasons before the experiment was completed. No surviving mice were excluded from the analysis. For the treatment of established tumors, mice were injected with FT-t cells as described above. Seven days later, 2 mice were sacrificed and examined for the presence of tumors. Tumors were observed visually and were confirmed by histology. Treatment with vehicle or the combination of erastin and A939572 was then initiated in the remaining mice ($n = 5$/group) and continued as described above until sacrifice at day 18.

Animal ethics statement

Animal studies were conducted in accordance with the recommendations in the Guide for the Care and Use of Laboratory Animals of the Association for Assessment and Accreditation of Laboratory Animal Care International. The experimental protocol was approved by the Institutional Animal Care and Use Committee at the University of Connecticut Health Center (protocol #100881).

Statistical analysis of cell culture experiments

Statistical analyses were performed using Excel or Prism 6 (GraphPad software). All experiments were performed at least 3 times using a minimum of 3 replicates per condition in each experiment. Comparison tests were performed between two groups, and statistical significance was assessed using two-tailed unpaired Student *t* tests. Statistics are reported as the mean ± standard deviation.

Database analyses

Publicly available Affymetrix GeneChip U133A Plus 2.0 expression profile array of laser-capture microdissected normal fallopian epithelial cells (with and without known *BRCA1/2* mutations) and high-grade serous ovarian or fallopian epithelial cells (GEO accession no. GSE109071) were preprocessed as described (18). Preprocessed The Cancer Genome Atlas (TCGA) Affymetric GeneChip U133A expression profile array data were obtained from the curated OvarianData database (19). Further analysis of these data sets was performed as described in Supplementary Materials and Methods.

Fatty acid methyl ester analysis and lipidomics

Fatty acid methyl ester (FAME) analysis was performed using GC-MS, and untargeted lipidomics analysis was performed using ultra high-performance liquid chromatography–tandem mass spectrometry (UHPLC-MS). Details are provided in Supplementary Materials and Methods.

Results

SCD1 is overexpressed across histologic and molecular subtypes of ovarian cancer and in a genetic model of ovarian cancer stem cells

We first assessed the expression of SCD1 in ovarian cancer. There are multiple histologic subtypes of ovarian cancer, including adenocarcinoma, endometriod, and HGSOC. We tested whether SCD1 was broadly upregulated across these ovarian cancer subtypes using representative cell lines. As shown in Fig. 1A and B, when compared with normal HOSE cells, there was an increase in both levels of SCD1 mRNA and protein in all but one ovarian cancer cell line tested. Although the extent of upregulation was variable, there was a general concordance between levels of mRNA and protein, suggesting that the increase in SCD1 is transcriptionally driven. Analysis of a publicly available gene-expression database (GEO accession GSE109071) demonstrated that *SCD* was similarly elevated in samples from patients with HGSOC (Fig. 1C). Consistent with these results, IHC analysis revealed that SCD1 protein was increased in tumors from patients with HGSOC when compared with nonmalignant ovarian epithelium (Fig. 1D; Supplementary Fig. S1).

We also examined SCD1 in a genetic model of ovarian cancer stem cells created by introduction of h*TERT*, SV40 large T, and *c-myc* into normal human fallopian stem cells (12). Cells of the fallopian tube represent at least one of the precursor cells for ovarian cancer (20), and we have previously shown that these FT-t cells form tumors with the characteristic features of HGSOC (12). SCD1 was similarly elevated in these FT-t cancer stem cells when compared with immortalized but not transformed fallopian stem cells (FT-i; Fig. 1A and B).

Ovarian cancer has been divided into prognostic subtypes based on gene-expression profile (21). Subtypes identified were proliferative, differentiated, immunoreactive, and mesenchymal (21). To test whether *SCD* was differentially expressed in ovarian cancer subtypes, we queried TCGA database. As shown in Fig. 1E, levels of *SCD* transcripts differed across subtypes, with the highest level observed in the mesenchymal subtype. The mesenchymal phenotype has been broadly associated with stem cell characteristics and with sensitivity to ferroptosis inducers in other cancers (22, 23).

Inhibition of SCD1 induces ferroptotic cell death

The high levels of expression of SCD1 in ovarian cancer cells suggested that SCD1 may play an important role in these cells. To

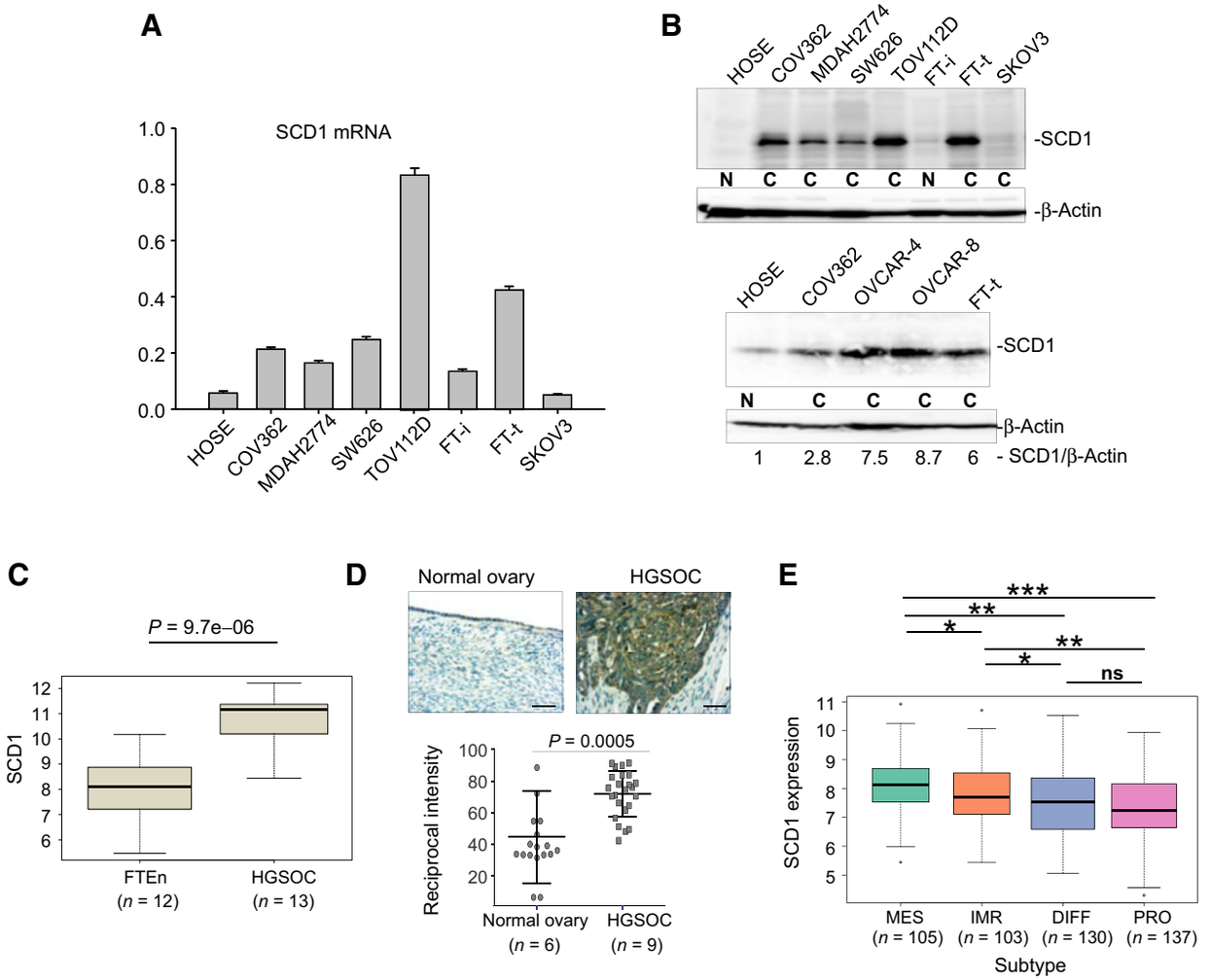

Figure 1.

SCD1 is upregulated in ovarian cancer. **A,** SCD1 mRNA in multiple ovarian cancer cell lines and normal ovarian cells assessed using qRT-PCR. [FT-i, immortalized fallopian tube cells; FT-t, transformed fallopian tube cells (cancer stem cells, see ref. 9)]. **B,** Western blot analysis of SCD1 in ovarian cells. N, nonmalignant cell lines; C, ovarian cancer cell lines. Histologic subtypes represented by these cell lines are as follows: adenocarcinoma, SW626, SKOV3; endometriod, MDAH2774, TOV112D; HGSOC, COV362, OVCAR4, OVCAR8. **C,** Expression of SCD1 in GEO (GSE 109071). HGSOC compared with normal fallopian tube epithelium (FTEn). **D,** IHC staining of SCD1 in patient tissues. Scale bar, 100 μm. Top, representative image of normal ovary and HGSOC; bottom, staining quantification (normal ovary $n = 6$; HGSOC $n = 9$). Two to three different images were captured per patient slide and quantified. Dot plot depicts means and SDs of 17 images of normal tissues and 23 images of HGSOC patient tissues. **E,** Differences in *SCD1* expression in prognostic TCGA subtypes. MES, mesenchymal; IMR, immunoreactive; DIFF, differentiated; PRO, proliferative. Boxes represent first and third quartiles, line is median, whiskers indicate data spread, and outliers are represented by dots. Width of boxes is proportional to sample size. *, $P < 0.05$; **, $P < 1.0E{-}03$; ***, $P = 1.2E{-}E07$.

test this hypothesis, we inhibited SCD1 using MF-438 and CAY10566, two chemically distinct pharmacologic inhibitors of SCD1 enzymatic activity. As shown in Fig. 2A–E, treatment of OVCAR4 HGSOC cells, as well as ovarian cancer stem cells, FT-t, with MF-438 and CAY10566 for 72 hours reduced cell viability and increased cell death. Viability was restored by providing cells with oleic acid, one of the endproducts of SCD1 activity. Consistent with the higher levels of SCD1 in FT-t cells compared with FT-i cells, FT-t cells were more sensitive to SCD1 inhibitors than FT-i cells (Supplementary Fig. S2). Cell death was also reduced by treatment with Fer-1, an inhibitor of ferroptosis, suggesting that reduction of SCD1 activity induces cell death at least in part by triggering ferroptosis. Consistent with this interpretation, treatment with an SCD1 inhibitor increased lipid oxidation, a characteristic feature of ferroptosis (Fig. 2F). To confirm and expand these results beyond a single ovarian cancer cell line, we inhibited SCD1 in COV362 cells using siRNA (Supplementary Fig. S3A) and measured effects on cell viability. As shown in Fig. 3A and B, knockdown of *SCD* reduced cell viability in both COV362 ovarian cancer cells and ovarian cancer stem cells. Viability was restored by providing cells with either oleic acid or Fer-1, confirming that SCD1 prevents ferroptotic cell death in both ovarian cancer cells and ovarian cancer stem cells.

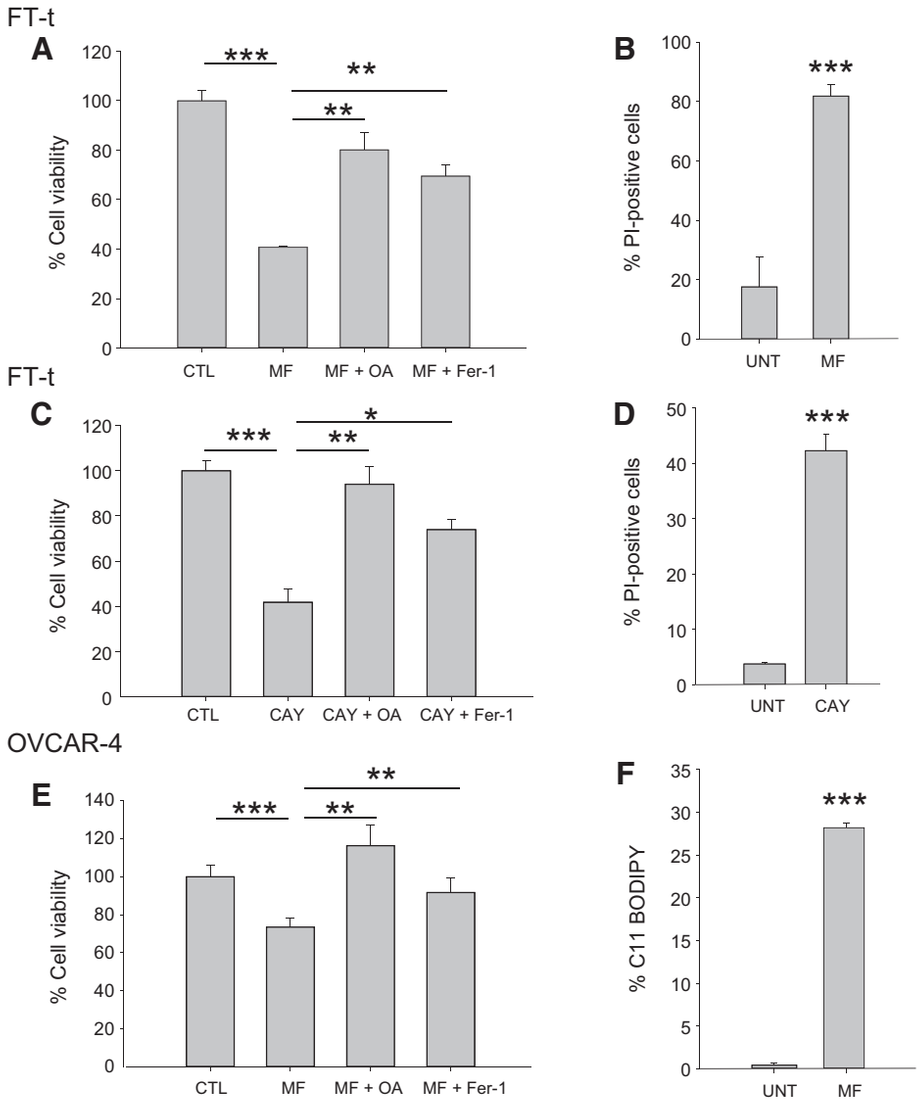

Figure 2.

Blocking SCD1 activity using small-molecule inhibitors causes cell death that can be rescued by oleic acid and the ferroptosis inhibitor Fer-1. Cells were treated with 1 μmol/L MF-438 (MF) or 5 μmol/L CAY10566 (CAY) in the presence or absence of 5 μmol/L Fer-1 or 80 μmol/L oleic acid (OA) for 48 to 72 hours. Cell viability was assessed by calcein-AM (**A, C,** and **E**), and cell death was assessed using propidium iodide (**B** and **D**). **F,** C11-BODIPY staining of OVCAR-4 cells following treatment with 1 μmol/L RSL3 in the presence or absence of 2 μmol/L Fer-1 for 2 hours. Experiments are representative of three independent experiments. Shown are means and SD of 8 replicates in one representative experiment. *, $P < 2E{-}04$; **, $P < 6E{-}05$; ***, $P < 4E{-}06$.

Expression of SCD1 protects cells from ferroptosis by increasing the formation of monounsaturated fatty acids

To further probe the influence of SCD1 on ferroptotic cell death, we performed the converse experiment by overexpressing *SCD* in HGSOC and ovarian cancer stem cells. As seen in Figs. 3C and D and 4A and B, overexpression of *SCD* led to a dramatic protection from ferroptotic cell death induced by RSL3 or erastin.

Because the formation of oxidized membrane PUFAs is a hallmark of ferroptosis, we next asked whether SCD1 prevented ferroptotic cell death by preventing the formation of these lipid species. *SCD* overexpressing and control cells were treated with RSL3, and lipid oxidation measured by staining with C11-BODIPY, a dye that detects lipid ROS in cell membranes. This experiment demonstrated a significant decrease in oxidized lipids in cells overexpressing SCD1 (Fig. 4C–E).

Consistent with these results, cell death triggered by exposure to the ferroptosis inducer RSL-3 could be rescued by supplementation with palmitoleic or oleic acid, two products of SCD1 activity (Fig. 5A and B). Rescue was specific to monounsaturated fatty acids (MUFA), and could not be recapitulated with palmitic or stearic acid, the corresponding saturated fatty acids (Fig. 5C and D). In fact, exposure to these saturated fatty acids was toxic in itself (Fig. 5C–F). In contrast to results with MUFAs, the toxic effect of saturated fatty acids could not be inhibited by Fer-1, but could successfully be rescued by zVAD-fmk, an inhibitor of apoptosis (Fig. 5E and F).

Work from other groups has shown that blockade of SCD1 induces apoptosis (24, 25). We sought to reconcile these findings with our observations that inhibition of SCD1 induces ferroptosis. We therefore treated cells with the combination of an SCD1 inhibitor and zVAD-fmk, an apoptosis inhibitor, or Fer-1, a ferroptosis inhibitor. As shown in Fig. 5G, the decrease in cell viability caused by inhibition of SCD1 could be partially rescued by either zVAD-fmk or Fer-1 but not by necrostatin, an inhibitor of necrosis (Fig. 5G). This observation suggests that inhibition of SCD1 triggers two specific death pathways, apoptosis and ferroptosis. To support these findings, we measured caspase activation, a specific marker of apoptosis, following inhibition of SCD1.

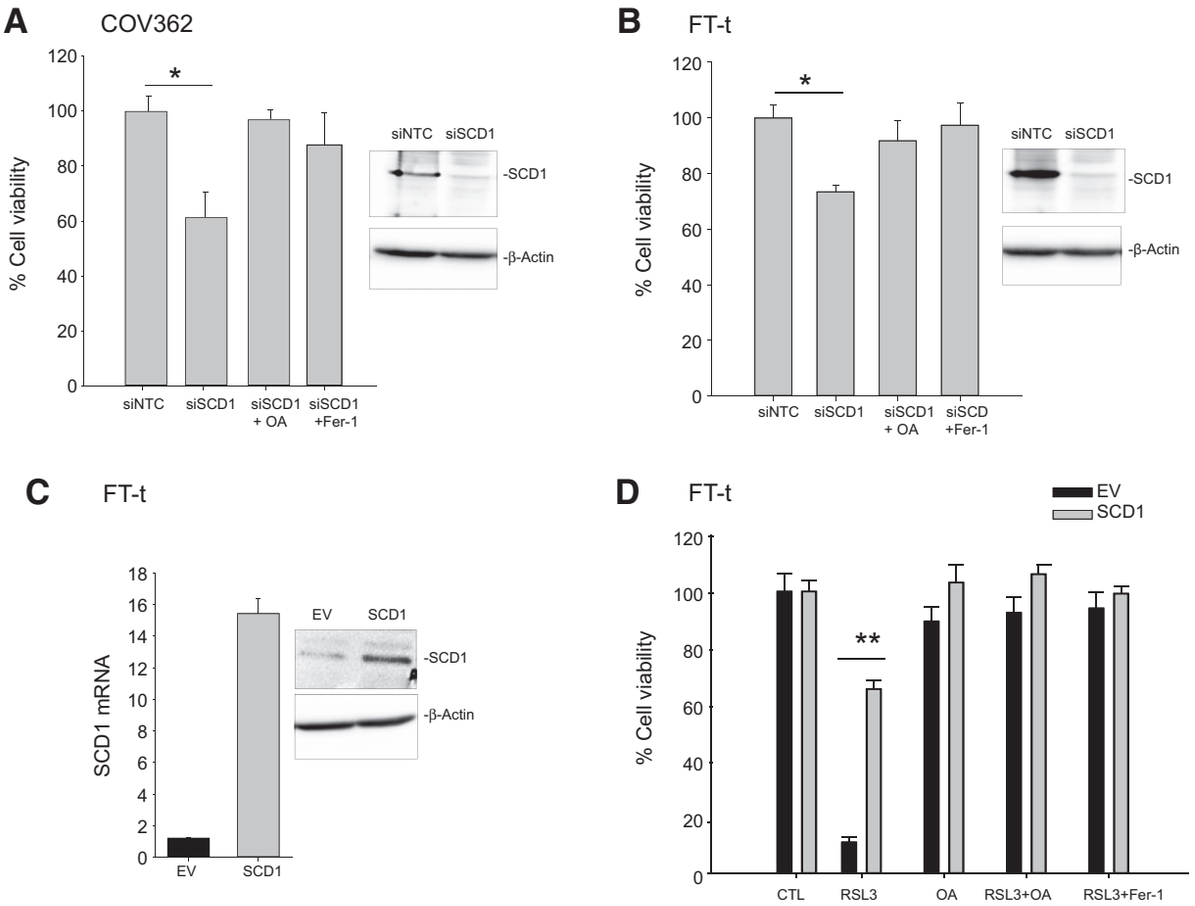

Figure 3.

Modulation of SCD1 affects ferroptosis in ovarian cancer cells. **A** and **B,** COV362 (**A**) and FT-t (**B**) cells were transfected with siRNA targeted to SCD1 (siSCD1) or nontargeting siRNA (siNTC) for 72 hours in the presence and absence of 5 μmol/L Fer-1 or 80 μmol/L oleic acid (OA). **C,** Expression of SCD1 in Tet-on constructs analyzed using RT-qPCR and Western blotting. EV, empty vector. **D,** FT-t cells overexpressing SCD1 or empty vector controls were treated with 5 μmol/L RSL3 in the presence or absence of 10 μmol/L Fer-1 or 80 μmol/L oleic acid for 24 hours, and viability was measured. Graphs are representative of four independent experiments. Shown are means and SDs of 8 replicates in one representative experiment. *, $P < 2.5E{-}07$; **, $P < 5.3E{-}11$.

Staurosporine, a known inducer of apoptosis, was used as a positive control. As shown in Fig. 5H, inhibition of SCD1 increased caspase activity, consistent with induction of apoptosis. Further, combined treatment with zVAD-fmk and Fer-1 almost completely blocked cell death (Fig. 5G), indicating that ferroptosis and apoptosis are the principal modes of cell death induced by inhibition of SCD1.

Mechanistic links between SCD1, ferroptosis, and apoptosis

We next explored mechanisms by which SCD1 inhibition triggers dual cell death pathways. We focused on lipid metabolism due to the biochemical properties of SCD1 and its known role in lipid remodeling (7). Lipids have been linked to both apoptosis and ferroptosis. Ceramides are apoptosis mediators (26, 27), whereas oxidized PUFAs mediate ferroptosis (2). Further, the mevalonate pathway, particularly CoQ_{10}, has been implicated in protection from ferroptosis (6). We therefore probed changes in lipid composition induced by SCD1 blockade using both an analysis of fatty acid composition (FAME analysis) and ultra-performance liquid chromatography/tandem mass spectrometry (UHPLC-MS), a global untargeted lipidomic analysis of major lipid classes.

We first confirmed that perturbation of SCD1 had the anticipated downstream consequences on fatty acid composition. In particular, SCD1 catalyzes the formation of a double bond in the cis-Δ9 position of saturated fatty acyl-CoAs, particularly palmitoyl CoA and stearolyl CoA (C16:0 and C18:0), to produce the monounsaturated fatty acids palmitoleate and oleate (C16:1 and C18:1, respectively). Inhibition of this reaction would therefore be expected to decrease the ratio of monounsaturated to saturated fatty acids. To confirm this we performed FAME analysis. *SCD* knockdown indeed caused an overall decrease in the ratio of 16:1/16:0 and 18:1/18:0 monounsaturated/saturated fatty acids (average decrease of 55% ± 7% and 38% ± 17%, respectively).

To clarify and distinguish the roles of SCD1 in apoptosis and ferroptosis, we next investigated effects of *SCD* knockdown on overall lipid composition using an untargeted lipidomic analysis that compared relative levels of over 1,700 individual lipid species, including ceramides, phospholipids, free fatty acids, and

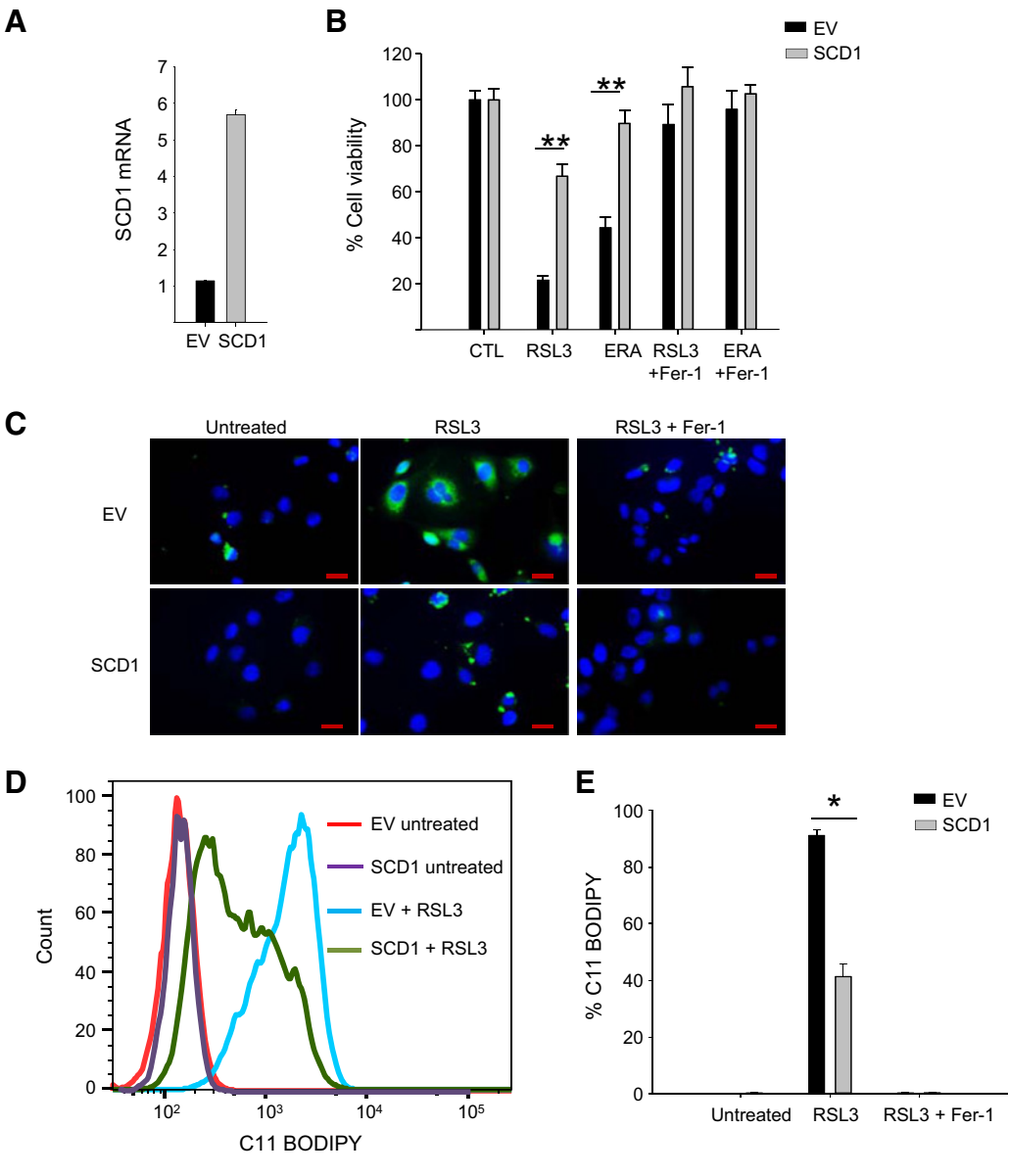

Figure 4.

Overexpression of SCD1 protects cells from RSL3-mediated lipid peroxidation. **A,** SCD1 mRNA in COV362 cells constitutively overexpressing SCD1 (SCD1) or empty vector control (EV) measured by RT-qPCR. **B,** Viability of COV362 cells overexpressing SCD1 or empty vector controls following treatment with 5 μmol/L RSL3 or 5 μmol/L erastin in the presence or absence of 10 μmol/L Fer-1 for 48 hours. **C,** C11-BODIPY staining of COV362 SCD1 and COV362 EV cells following treatment with 5 μmol/L RSL3 in the presence or absence of 2 μmol/L Fer-1 for 4 hours. Blue, DAPI; green, C11 BODIPY. Scale bar, 20 μm. **D,** C11-BODIPY staining analyzed by flow cytometry. **E,** Quantification of C11-BODIPY–positive cells. Means and SD on of at least three replicas. *, $P < 5.5E{-}05$; **, $P < 3.7E{-}9$.

triglycerides, in cells that had been treated with three chemically distinct inhibitors of SCD1.

We first noted that consistent with our FAME analysis, the ratio of SFA/MUFA increased across all lipid classes with SCD1 inhibition (Fig. 6A). Among lipids that increased with SCD1 inhibition (i.e., that were positively associated with SCD1-mediated cell death), the most notable were ceramides containing saturated fatty acids (Fig. 6B). An increase in long-chain saturated ceramide levels has previously been linked to apoptotic cell death (24), consistent with our observation that SCD1 inhibition induces apoptosis (Fig. 5G and H). We also observed a decrease in membrane phospholipids containing unsaturated fatty acids (Fig. 6C), a change that has also been linked to apoptosis in cells deprived of SCD1 (28). These results implicate SCD1-mediated effects on ceramides and saturation of phospholipid acyl chains as likely contributors to apoptotic cell death in ovarian cancer cells depleted of SCD1.

Ferroptotic cell death has been linked to oxidation of PUFAs, particularly PE containing arachidonic acid (C20:4) and adrenic acid (C22:4; refs. 2, 29). We therefore asked whether arachidonic or adrenic acid increased following SCD1 inhibition. However, we noted no increase in either free arachidonic acid (adrenic

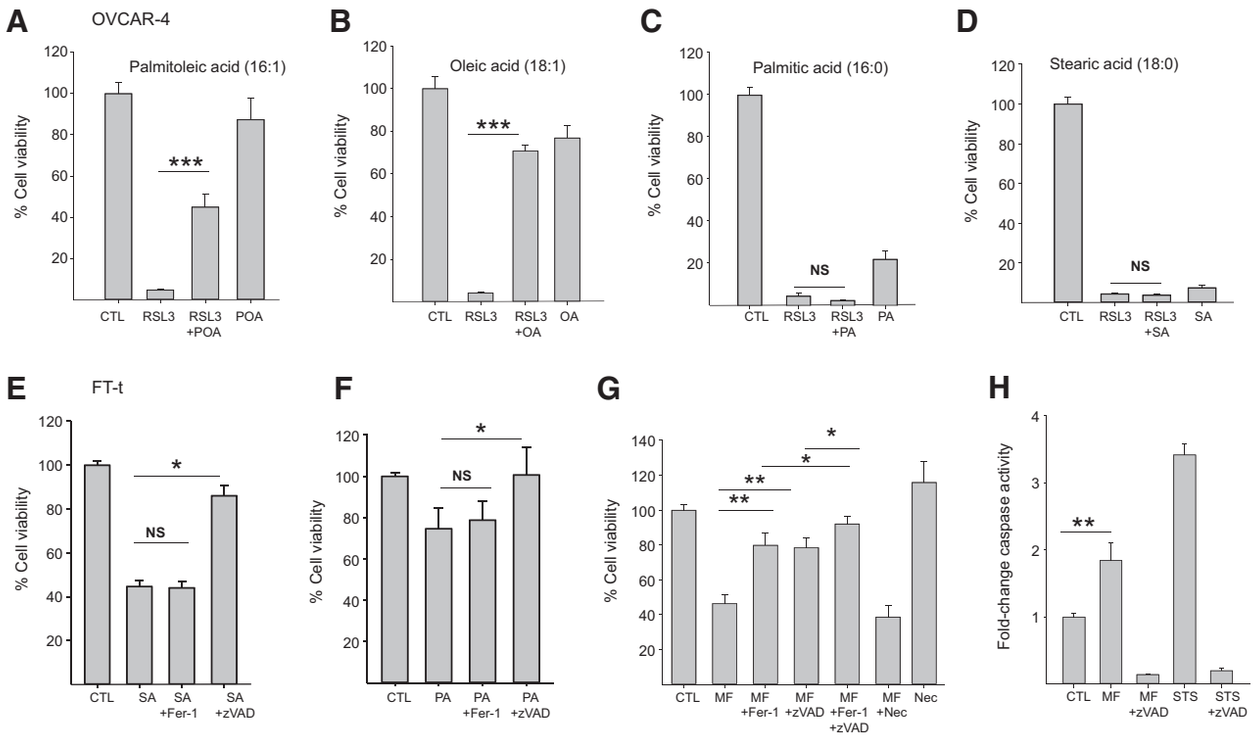

Figure 5.

Effects of exogenous lipids, death pathway inhibitors, and SCD1 inhibitors on viability and caspase activity in ovarian cancer cells and ovarian cancer stem cells. **A–D,** Viability of OVCAR-4 cells treated with 2 μmol/L RSL3 in the presence or absence of 80 μmol/L of the indicated lipids for 24 hours. **E** and **F,** Viability of FT-t cells treated with 80 μmol/L stearic acid (SA) or palmitic acid (PA) in the presence or absence of 10 μmol/L zVAD-fmk or 5 μmol/L Fer-1 for 24 hours. **G,** Viability of FT-t cells treated with 10 μmol/L MF-438 in the presence or absence of 5 μmol/L Fer-1, 10 μmol/L zVAD-fmk, or 10 μmol/L necrostatin for 48 hours. **H,** Relative caspase-3/7 activity in FT-t cells treated with 10 μmol/L MF-438 for 48 hours or 1 μmol/L staurosporin for 4 hours in the presence or absence of 10 μmol/L zVAD-fmk. Data shown are representation of at least three independent experiments. Graphs are means and SD of 8 replicas in one representative experiment. *, $P < 0.024$; **, $P < 1E{-}04$; ***, $P < 7E{-}14$. NS, nonsignificant.

acid was not detected); arachidonoyl- or adrenoyl-esterified PE; or arachidonic and adrenic acid–containing lipids of any class (Supplementary Table S1). In fact, the converse appeared true—arachidonic and arachidonic acid-containing lipids either remained unchanged or tended to decrease following SCD1 inhibition (Supplementary Table S1). This may reflect the oxidative destruction of these species during ferroptosis (29).

We next explored the possibility that downregulation of SCD1 might induce ferroptosis by decreasing synthesis of cytoprotective lipids. CoQ_{10} is an endogenous antioxidant produced by the mevalonate pathway. Depletion of CoQ_{10} has previously been linked to ferroptosis triggered by the synthetic ferroptosis inducer FIN56 (6). As shown in Fig. 6D, after downregulation of SCD1 we observed a striking reduction of the lipophilic antioxidant coenzyme Q_{10}.

Collectively, these results are consistent with a model in which SCD1 depletion triggers apoptosis by increasing synthesis of ceramides enriched in saturated fatty acids and altering the ratio of saturated to unsaturated fatty acids, whereas ferroptosis is triggered by depleting CoQ_{10}.

Blocking SCD1 sensitizes ovarian cancer cells to ferroptosis inducers *in vitro* and *in vivo*

The effects of SCD1 on lipid metabolism suggested that inhibition of SCD1 might potentiate the cytotoxic effect of ferroptosis inducers. To test this prediction, we pretreated both ovarian cancer stem cells and ovarian tumor cells with two different SCD1 inhibitors for short periods of time, with the aim of inducing only modest toxicity. We then assessed sensitivity to RSL3 and erastin, two ferroptosis inducers that act at different steps in the ferroptosis cascade (1). Pretreatment of both ovarian cancer stem cells and ovarian tumor cells with the SCD1 inhibitors MF-438, CAY10566, or A939572 dramatically sensitized cells to RSL3 (Fig. 7A–C) and erastin (Supplementary Fig. S3B). Combined treatment with SCD1 inhibitors and RSL3 resulted in a synergistic cytotoxic effect on FT-t cells as calculated by the Chou–Talalay method (Supplementary Fig. S4; ref. 16). The decrease in viability in cells treated with the combination of RSL3 and SCD1 inhibitors was characterized by an increased oxidation of membrane lipids (Fig. 7D), consistent with an increase in ferroptotic cell death. Further, blockade of *SCD* using siRNA or shRNA similarly sensitized cells to RSL3 (Supplementary Fig. S5), ruling out nonspecific effects of SCD1 inhibitors on ferroptosis sensitization. A similar augmentation of erastin cytotoxicity was observed using the SCD1 inhibitor A939572 (Fig. 7E). We also tested the sensitivity of OVCAR8 and OVCAR5 cells, two cell lines representative of the mesenchymal subtype of ovarian cancer (30, 31) to the combination of a ferroptosis inducer and SCD1 inhibitor. As shown in Supplementary Fig. S6A, both these cells exhibited

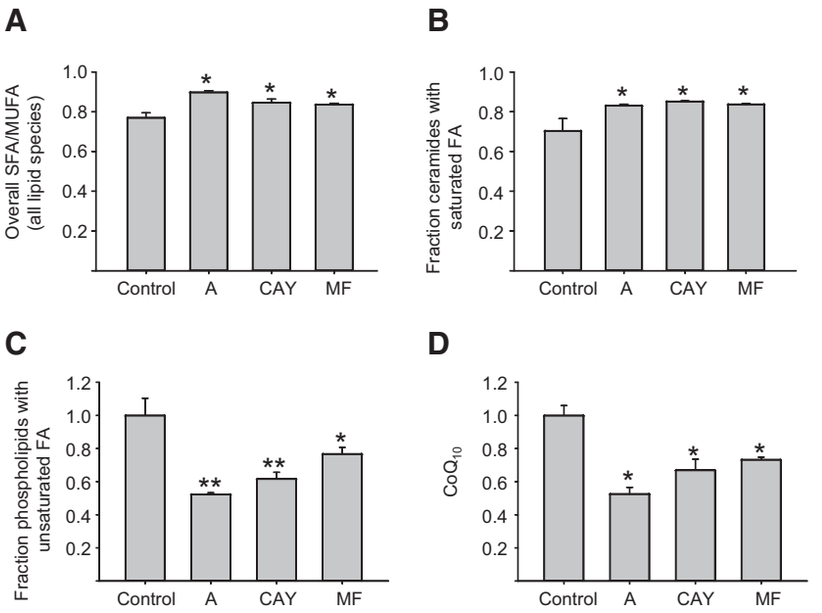

Figure 6.

Inhibition of SCD1 modulates lipid content of ovarian cancer cells. FT-t cells were treated in triplicate with vehicle (control) or three chemically unrelated, commercially available SCD1 inhibitors, A939572 (A), CAY10566 (CAY), and MF-438 (MF), for 72 hours prior to harvest for untargeted lipid analysis by UHPLC-MS. **A,** Ratio of saturated/monounsaturated fatty acids in all lipid species. **B,** Fraction of ceramides with saturated fatty acids. **C,** Fraction of phospholipids with unsaturated fatty acids. **D,** Levels of coenzyme Q10. Means and SDs of triplicate determinations are shown. *, $P < 0.04$; **, $P < 0.01$.

an enhanced response to a ferroptosis inducer following pharmacologic inhibition of SCD1.

To test whether blockade of SCD1 could potentiate the antitumor effects of ferroptosis inducers *in vivo*, we induced ovarian tumors in mice by injecting ovarian cancer stem cells into the peritoneal cavity, as we have previously described (9). The next day, mice were treated with either vehicle alone, erastin alone, the SCD1 inhibitor A939572 alone, or the combination of erastin and A939572. Mice were sacrificed after 18 days, and tumor number and weight were assessed. As shown in Fig. 7, inhibition of SCD1 exerted substantial antitumor effects on its own and significantly potentiated the antitumor effect of erastin, reducing both tumor number (Fig. 7F) and tumor mass (Fig. 7G) when compared with erastin treatment alone. We next examined whether this drug combination was also effective in established tumors. Following tumor cell injection, tumors were allowed to grow for 7 days, which is approximately a third of the total time required for the development of ascites, morbidity, and death in this model. We sacrificed 2 mice and confirmed that peritoneal tumors were present using visual examination and histologic evaluation. We then initiated combination with the combination of a ferroptosis inducer and SCD1 inhibitor (or vehicle control) in the remaining mice ($n = 5$/group). This treatment remained highly effective even in this more challenging experimental scenario, resulting in a statistically significant 6-fold decrease in tumor number ($P < 0.028$) and 5-fold decrease in total tumor mass ($P \leq 0.026$) compared with controls (Supplementary Fig. S6B).

Discussion

Ovarian cancer is often diagnosed late, and few good therapeutic options exist (32). The discovery of ferroptosis, a mechanism of cell death to which ovarian cancer cells are susceptible (9), opens the door to new treatments for this disease. In this article, we report that SCD1 is overexpressed in ovarian cancer, that genetic or pharmacologic blockade of SCD1 induces ferroptosis as well as apoptosis, and that blockade of SCD1 enhances sensitivity to ferroptosis inducers both in a genetic model of ovarian cancer stem cells and in ovarian cancer cell lines. Sensitization to ferroptosis inducers was observed both *in vitro* and *in vivo*.

Lipids participate in complex ways in multiple death pathways, acting as both initiators and facilitators of apoptosis, and impacting necroptosis and ferroptosis (27). Lipid oxidation appears to be particularly central to the process of ferroptosis. We observed that interference with lipid homeostasis through blockade of SCD1 induced multiple changes in cellular lipid content. In addition to lipid oxidation (Figs. 4 and 7) we observed an increase in apoptosis-promoting ceramides and a decrease in the lipid antioxidant coenzyme Q10 (Fig. 6). These complex changes conspire to induce two death pathways, ferroptosis and apoptosis, in ovarian cancer cells challenged with SCD1 inhibitors (Fig. 5). Simultaneous triggering of two death pathways suggests SCD1 inhibition may be a particularly effective component of antitumor therapy, because overcoming this dual mechanism of cell death may present a significant barrier to the emergence of drug resistance.

SCD1 may be regulated through one or more of the complex pathways that link tumor suppressors to ferroptosis (33). For example, p53 (*TP53*) has been shown to repress SCD1 (34). Based on our findings, repression of *SCD* might contribute to the tumor-suppressive activity of p53 by disabling the antiferroptotic function of SCD1. This would be consistent with work by others that has shown that in lung cancer, osteosarcoma, and breast cancer, p53 sensitizes cells to ferroptosis by repressing SLC7A11, a cystine/glutamate antiporter required for the synthesis of GSH and the activity of GPX4 (35). However, the role of p53 is complex, and in colorectal cancer, p53 antagonizes rather than fosters ferroptosis by blocking DPP4 activity (36). Further, recent work has shown that effects of p53 may also depend on its ability to induce p21 (*CDKN1A*; ref. 37). BRCA/associated protein 1 (BAP1), another potent tumor suppressor, has also been linked to ferroptosis (38, 39), although a connection between BAP1 and

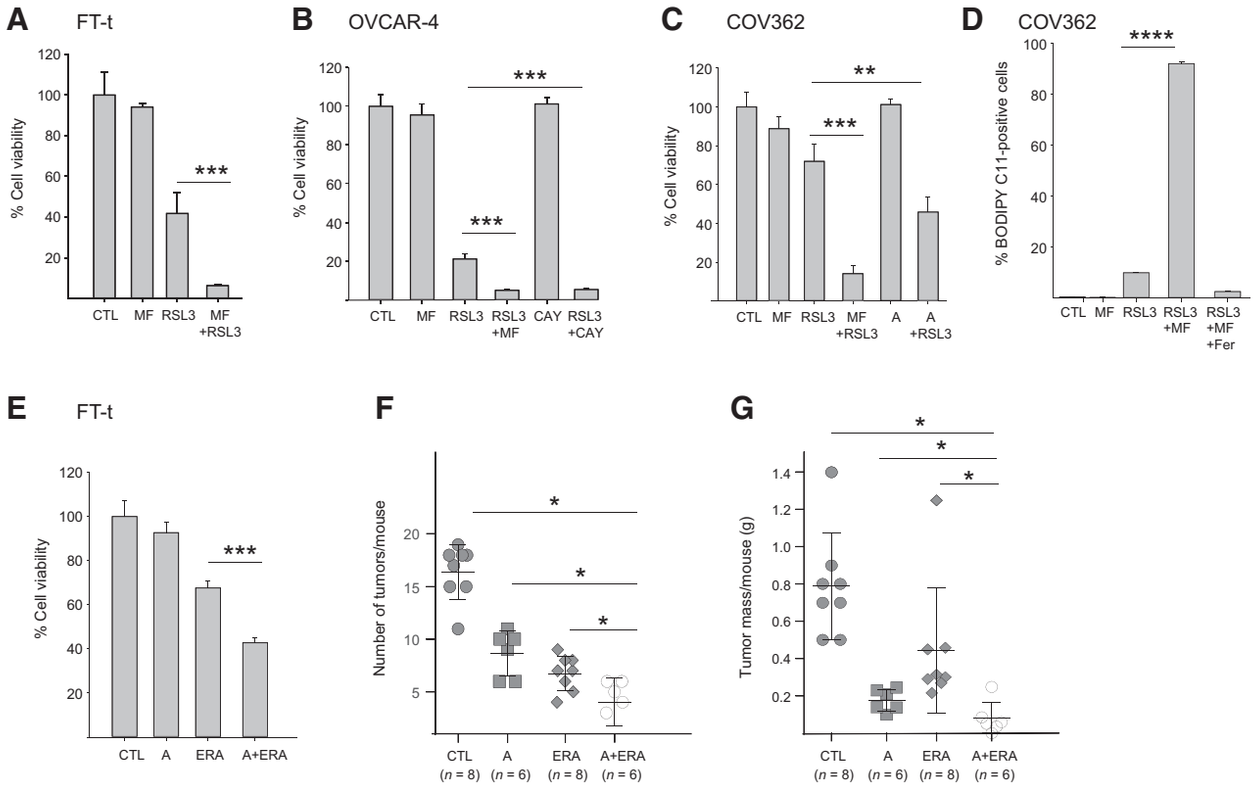

Figure 7.

Blocking the activity of SCD1 with small-molecule inhibitors increases lipid peroxidation, ferroptotic cell death, and the antitumor effect of a ferroptosis inducer *in vivo*. **A–C,** Viability of FT-t (**A**), COV362, or OVCAR-4 cells pretreated with 1 μmol/L MF-438 (MF), 1 μmol/L CAY10566 (CAY), or 5 μmol/L A939572 (A) for 24 hours, followed by the addition of RSL3 for an additional 24 hours. For each cell type, dose of RSL3 was adjusted to attain modest cytotoxicity in the absence of SCD1 inhibitors (FT-t, 2 μmol/L RSL3; OVCAR-4, 1 μmol/L RSL3; COV362, 5 μmol/L RSL3). Control cells were treated with SCD1 inhibitor for 48 hours or RSL3 for 24 hours. Data shown are representative of at least three independent experiments each with 8 to 12 replicas, **D**, C11-BODIPY staining of COV362 cells treated with 1 μmol/L MF-438 for 24 hours, followed by 1 μmol/L RSL3 for 4 hours in the presence or absence of Fer1. **E,** Viability of FT-t cells treated with A939572 (A) alone, 1 μmol/L erastin (ERA) alone, or A939572 followed by erastin. Graphs are representative of at least three independent experiments, each with 3 to 8 replicas. **F** and **G,** Mice were injected i.p. with FT-t cells and treated for 18 days with either vehicle control, A939572 (A), erastin (ERA) or the combination of A939572 and erastin. **F**, The number of tumors/mouse. **G,** Total tumor mass/mouse. *, $P < 0.04$; **, $P < 0.00027$; ***, $P < 2E{-}05$; ****, $P < 7.2E{-}10$.

SCD1 has not yet been established. Dissecting the multiple links between tumor suppressors, SCD1 and ferroptosis, promises to be a fruitful avenue for further investigation.

We propose a model for the mechanism by which SCD1 blockade potentiates effects of ferroptosis inducers. We hypothesize that inhibiting SCD1 alters membrane phospholipid composition, decreasing the content of monounsaturated fatty acyl chains at the expense of increased polyunsaturated fatty acyl chains, as well as decreasing membrane-localized antioxidants (Fig. 6). This shift in membrane composition provides more substrate for membrane lipid oxidation, thus sensitizing cells to ferroptosis inducers, which trigger cell death by increasing lipid oxidation (Figs. 4 and 7). Induction of apoptosis through modulation of ceramide content further contributes to the antitumor effect of combined SCD1 blockade and ferroptosis induction (Fig. 6).

In contrast to our finding that inhibition of SCD1 causes cell death in ovarian cancer cells, others have reported that SKOV3 cells are relatively insensitive to cell death induced by SCD1 blockade (24). There are two potential explanations for this discrepancy. First, although the SKOV3 cell line is used to model HGSOC, the validity of this cell line as a model of HGSOC has been questioned on the basis of genomic profiling (40). Thus, it is unclear that results obtained with SKOV3 cells (which may be representative of a different histologic subtype of ovarian cancer; ref. 40) should be expected to be concordant with results reported here, which are based on OVCAR 4 and COV362 cell lines, which exhibit genetic as well as histologic features that approximate HGSOC (40, 41). Second, we noted that the SKOV3 cell line expresses the lowest level of SCD1 of all the ovarian cancer cell lines we tested (Fig. 1), suggesting that SKOV3 cells may be less dependent on this pathway than other ovarian cancer cells, and consequently less sensitive to its inhibition.

There are several promising features of the use of SCD1 inhibitors as an adjunct to ferroptosis inducers in ovarian cancer therapy. First, SCD1 inhibitors can inhibit MUFA formation despite the presence of other SCD isoforms, although SCD5 is also expressed in humans, it appears unable to compensate for the loss of SCD1 (42).

Second, it may be possible to manage systemic toxicities engendered by SCD1 blockade. SCD1 knockout mice are viable, suggesting that normal tissues can tolerate long-term loss of SCD1 function (43). However, knockout mice do exhibit toxicities, including fur loss, skin abnormalities, and weight reduction, effects that

closely mimic effects in mice treated long term with candidate SCD1 inhibitors (44). These side effects have presented an obstacle to the development of SCD1 inhibitors as obesity drugs, shifting attention to their use in oncology (45). Use of SCD1 inhibitors in a more temporally and spatially restricted manner in cancer treatment may be feasible, both because these side effects, which appear linked to sustained SCD1 inhibition, may be less evident with shorter term cancer treatments, and because in ovarian cancer patients, delivery of drugs to the peritoneal cavity, close to the site of the tumor, is a clinically viable option that may reduce drug exposure of peripheral organs and therefore undesired side effects (46). Finally, the use of SCD1 inhibitors in combination with a ferroptosis inducer may allow use of lower doses of both agents, with consequent reduction in systemic toxicity. For example in our experiments, we observed augmentation of RSL3 cytotoxicity with concentrations of A 939572, CAY10566, or MF-438 that under the same conditions exhibited minimal effects as single agents (Fig. 7).

Third, anticancer drugs that induce ferrroptosis are currently available. These include sorafinib, a multikinase inhibitor (47), as well as drugs such as cisplatin, which was recently shown to trigger ferroptosis (48). Thus, although there is an intensive effort to develop new drugs to trigger ferroptosis, implementation of an anticancer approach that includes a ferroptosis inducer need not await new drug discovery.

Fourth, combined use of a ferroptosis inducer and SCD1 blockade is effective in inhibiting proliferation of cancer stem cells (Fig. 7). Using a genetic model of an ovarian cancer stem cell, we observed that inhibition of SCD1 was highly effective in inducing lipid oxidation and cell death *in vitro*, and in inhibiting tumor growth *in vivo* (Fig. 7). Because cancer stem cells are hypothesized to contribute to drug resistance and disease recurrence, and the emergence of drug resistance is a major contributor to the poor outcome of patients with ovarian cancer, eradicating these cells may be of particular clinical utility. Supporting this concept, inhibitors of GPX4 (i.e., ferroptosis inducers) were found to be particularly effective in targeting drug-resistant "persister" cells in tumors (22) as well as tumor cells with mesenchymal characteristics (23). We observed that two ovarian cancer cell lines representative of the mesenchymal subtype were sensitive to the combined effect of an SCD1 inhibitor and ferroptosis inducer (Supplementary Fig. S6A), suggesting that a therapeutic approach involving inhibition of SCD1 in combination with induction of ferroptosis may be of benefit even in this treatment-refractory subtype of ovarian cancer.

Overall, our results demonstrate that ovarian tumors express high levels of SCD1, and that blockade of SCD1 modulates lipid metabolism and sensitizes ovarian cancer cells to ferroptosis inducers *in vitro* and *in vivo*. Treatment of ovarian cancer with the combination of SCD1 inhibitors and ferroptosis inducers merits further investigation.

Note Added in Proof

While this article was under review, Magtanong and colleagues demonstrated that exogenous monounsaturated fatty acids promote a ferroptosis-resistant state (49).

Disclosure of Potential Conflicts of Interest

No potential conflicts of interest were disclosed.

Authors' Contributions

Conception and design: L. Tesfay, F.M. Torti, S.V. Torti
Development of methodology: L. Tesfay, B.T. Paul, Z. Deng, C.M. Furdui
Acquisition of data (provided animals, acquired and managed patients, provided facilities, etc.): A. Konstorum, A.O. Cox, J. Lee, C.M. Furdui
Analysis and interpretation of data (e.g., statistical analysis, biostatistics, computational analysis): L. Tesfay, B.T. Paul, A. Konstorum, A.O. Cox, J. Lee, F.M. Torti
Writing, review, and/or revision of the manuscript: L. Tesfay, A. Konstorum, Z. Deng, A.O. Cox, J. Lee, F.M. Torti, S.V. Torti
Study supervision: C.M. Furdui, S.V. Torti
Other (interpretation of immunohistochemistry, and editing the pertinent sections of the revised manuscript): P. Hegde

Acknowledgments

We thank Erica Lemler for her contribution to the early phases of this study and Dr. Evan Jellison for expert help in flow cytometry analysis. This study was supported by NCI grants R01 CA188025 (S.V. Torti), R01 CA171101 (F.M. Torti), F32CA214030 (A. Konstorum), and NCI Cancer Center Support Grant P30 CA012197 (Proteomics and Metabolomics Shared Resource at Wake Forest University Health Sciences).

The costs of publication of this article were defrayed in part by the payment of page charges. This article must therefore be hereby marked *advertisement* in accordance with 18 U.S.C. Section 1734 solely to indicate this fact.

Received January 31, 2019; revised June 4, 2019; accepted June 27, 2019; published first July 3, 2019.

References

1. Stockwell BR, Friedmann Angeli JP, Bayir H, Bush AI, Conrad M, Dixon SJ, et al. Ferroptosis: a regulated cell death nexus linking metabolism, redox biology, and disease. Cell 2017;171:273–85.
2. Kagan VE, Mao G, Qu F, Angeli JP, Doll S, Croix CS, et al. Oxidized arachidonic and adrenic PEs navigate cells to ferroptosis. Nat Chem Biol 2017;13:81–90.
3. Yang WS, Kim KJ, Gaschler MM, Patel M, Shchepinov MS, Stockwell BR. Peroxidation of polyunsaturated fatty acids by lipoxygenases drives ferroptosis. Proc Natl Acad Sci U S A 2016;113:E4966–75.
4. Doll S, Proneth B, Tyurina YY, Panzilius E, Kobayashi S, Ingold I, et al. ACSL4 dictates ferroptosis sensitivity by shaping cellular lipid composition. Nat Chem Biol 2017;13:91–8.
5. Dixon SJ, Winter GE, Musavi LS, Lee ED, Snijder B, Rebsamen M, et al. Human haploid cell genetics reveals roles for lipid metabolism genes in nonapoptotic cell death. ACS Chem Biol 2015;10:1604–9.
6. Shimada K, Skouta R, Kaplan A, Yang WS, Hayano M, Dixon SJ, et al. Global survey of cell death mechanisms reveals metabolic regulation of ferroptosis. Nat Chem Biol 2016;12:497–503.
7. Igal RA. Stearoyl CoA desaturase-1: new insights into a central regulator of cancer metabolism. Biochim Biophys Acta 2016;1861:1865–80.
8. Wang H, Klein MG, Zou H, Lane W, Snell G, Levin I, et al. Crystal structure of human stearoyl-coenzyme A desaturase in complex with substrate. Nat Struct Mol Biol 2015;22:581–5.
9. Basuli D, Tesfay L, Deng Z, Paul B, Yamamoto Y, Ning G, et al. Iron addiction: a novel therapeutic target in ovarian cancer. Oncogene 2017;36:4089–99.
10. Mai TT, Hamaï A, Hienzsch A, Cañeque T, Müller S, Wicinski J, et al. Salinomycin kills cancer stem cells by sequestering iron in lysosomes. Nat Chem 2017; DOI:10.1038/nchem.2778.
11. Li J, Condello S, Thomes-Pepin J, Ma X, Xia Y, Hurley TD, et al. Lipid desaturation is a metabolic marker and therapeutic target of ovarian cancer stem cells. Cell Stem Cell 2017;20:303–14.
12. Yamamoto Y, Ning G, Howitt BE, Mehra K, Wu L, Wang X, et al. In vitro and in vivo correlates of physiological and neoplastic human fallopian tube stem cells. J Pathol 2016;238:519–30.

13. Deng Z, Manz DH, Torti SV, Torti FM. Iron-responsive element-binding protein 2 plays an essential role in regulating prostate cancer cell growth. Oncotarget 2017;8:82231–43.
14. Blanchette-Farra N, Kita D, Konstorum A, Tesfay L, Lemler D, Hegde P, et al. Contribution of three-dimensional architecture and tumor-associated fibroblasts to hepcidin regulation in breast cancer. Oncogene 2018;37: 4013–32.
15. Crowley LC, Scott AP, Marfell BJ, Boughaba JA, Chojnowski G, Waterhouse NJ. Measuring cell death by propidium iodide uptake and flow cytometry. Cold Spring Harb Protoc 2016;2016. doi: 10.1101/pdb.prot087163.
16. Chou TC, Talalay P. Quantitative analysis of dose-effect relationships: the combined effects of multiple drugs or enzyme inhibitors. Adv Enzyme Regulation 1984;22:27–55.
17. Nguyen DH, Zhou T, Shu J, Mao J. Quantifying chromogen intensity in immunohistochemistry via reciprocal intensity. CancerInCytes 2013;2. Available at https://www.cancerincytes.org/quantifying-chromogen-intensity-in-immunohistochemistry-#!.
18. Konstorum A, Lynch ML, Torti SV, Torti FM, Laubenbacher RC. A systems biology approach to understanding the pathophysiology of high-grade serous ovarian cancer: focus on iron and fatty acid metabolism. OMICS 2018;22:502–13.
19. Ganzfried BF, Riester M, Haibe-Kains B, Risch T, Tyekucheva S, Jazic I, et al. curatedOvarianData: clinically annotated data for the ovarian cancer transcriptome. Database 2013;2013:bat013.
20. Kim J, Park EY, Kim O, Schilder JM, Coffey DM, Cho CH, et al. Cell origins of high-grade serous ovarian cancer. Cancers 2018;10. pii:E433.
21. Verhaak RG, Tamayo P, Yang JY, Hubbard D, Zhang H, Creighton CJ, et al. Prognostically relevant gene signatures of high-grade serous ovarian carcinoma. J Clin Invest 2013;123:517–25.
22. Hangauer MJ, Viswanathan VS, Ryan MJ, Bole D, Eaton JK, Matov A, et al. Drug-tolerant persister cancer cells are vulnerable to GPX4 inhibition. Nature 2017;551:247–50.
23. Viswanathan VS, Ryan MJ, Dhruv HD, Gill S, Eichhoff OM, Seashore-Ludlow B, et al. Dependency of a therapy-resistant state of cancer cells on a lipid peroxidase pathway. Nature 2017;547:453–7.
24. Chen L, Ren J, Yang L, Li Y, Fu J, Li Y, et al. Stearoyl-CoA desaturase-1 mediated cell apoptosis in colorectal cancer by promoting ceramide synthesis. Sci Rep 2016;6:19665.
25. Mason P, Liang B, Li L, Fremgen T, Murphy E, Quinn A, et al. SCD1 inhibition causes cancer cell death by depleting mono-unsaturated fatty acids. PLoS One 2012;7:e33823.
26. Obeid LM, Linardic CM, Karolak LA, Hannun YA. Programmed cell death induced by ceramide. Science 1993;259:1769–71.
27. Magtanong L, Ko PJ, Dixon SJ. Emerging roles for lipids in non-apoptotic cell death. Cell Death Differ 2016;23:1099–109.
28. Ariyama H, Kono N, Matsuda S, Inoue T, Arai H. Decrease in membrane phospholipid unsaturation induces unfolded protein response. J Biol Chem 2010;285:22027–35.
29. Doll S, Conrad M. Iron and ferroptosis: a still ill-defined liaison. IUBMB Life 2017;69:423–34.
30. Fang D, Chen H, Zhu JY, Wang W, Teng Y, Ding HF, et al. Epithelial-mesenchymal transition of ovarian cancer cells is sustained by Rac1 through simultaneous activation of MEK1/2 and Src signaling pathways. Oncogene 2017;36:1546–58.
31. Haley J, Tomar S, Pulliam N, Xiong S, Perkins SM, Karpf AR, et al. Functional characterization of a panel of high-grade serous ovarian cancer cell lines as representative experimental models of the disease. Oncotarget 2016;7:32810–20.
32. Lengyel E. Ovarian cancer development and metastasis. Am J Pathol 2010; 177:1053–64.
33. Gnanapradeepan K, Basu S, Barnoud T, Budina-Kolomets A, Kung CP, Murphy ME. The p53 tumor suppressor in the control of metabolism and ferroptosis. Front Endocrinol 2018;9:124.
34. Mirza A, Wu Q, Wang L, McClanahan T, Bishop WR, Gheyas F, et al. Global transcriptional program of p53 target genes during the process of apoptosis and cell cycle progression. Oncogene 2003;22:3645–54.
35. Jiang L, Kon N, Li T, Wang SJ, Su T, Hibshoosh H, et al. Ferroptosis as a p53-mediated activity during tumour suppression. Nature 2015;520: 57–62.
36. Xie Y, Zhu S, Song X, Sun X, Fan Y, Liu J, et al. The tumor suppressor p53 limits ferroptosis by blocking DPP4 activity. Cell reports 2017;20: 1692–704.
37. Tarangelo A, Magtanong L, Bieging-Rolett KT, Li Y, Ye J, Attardi LD, et al. p53 suppresses metabolic stress-induced ferroptosis in cancer cells. Cell Rep 2018;22:569–75.
38. Zhang Y, Shi J, Liu X, Feng L, Gong Z, Koppula P, et al. BAP1 links metabolic regulation of ferroptosis to tumour suppression. Nat Cell Biol 2018;20: 1181–92.
39. Affar EB, Carbone M. BAP1 regulates different mechanisms of cell death. Cell Death Dis 2018;9:1151.
40. Domcke S, Sinha R, Levine DA, Sander C, Schultz N. Evaluating cell lines as tumour models by comparison of genomic profiles. Nat Commun 2013;4: 2126.
41. Mitra AK, Davis DA, Tomar S, Roy L, Gurler H, Xie J, et al. In vivo tumor growth of high-grade serous ovarian cancer cell lines. Gynecol Oncol 2015; 138:372–7.
42. Flowers MT, Ntambi JM. Role of stearoyl-coenzyme A desaturase in regulating lipid metabolism. Curr Opin Lipidol 2008;19:248–56.
43. Ntambi JM, Miyazaki M, Stoehr JP, Lan H, Kendziorski CM, Yandell BS, et al. Loss of stearoyl-CoA desaturase-1 function protects mice against adiposity. Proc Natl Acad Sci U S A 2002;99:11482–6.
44. Zhang Z, Dales NA, Winther MD. Opportunities and challenges in developing stearoyl-coenzyme A desaturase-1 inhibitors as novel therapeutics for human disease. J Med Chem 2014;57:5039–56.
45. Theodoropoulos PC, Gonzales SS, Winterton SE, Rodriguez-Navas C, McKnight JS, Morlock LK, et al. Discovery of tumor-specific irreversible inhibitors of stearoyl CoA desaturase. Nat Chem Biol 2016;12:218–25.
46. Tewari D, Java JJ, Salani R, Armstrong DK, Markman M, Herzog T, et al. Long-term survival advantage and prognostic factors associated with intraperitoneal chemotherapy treatment in advanced ovarian cancer: a gynecologic oncology group study. J Clin Oncol 2015;33:1460–6.
47. Yang WS, Stockwell BR. Ferroptosis: death by lipid peroxidation. Trends Cell Biol 2016;26:165–76.
48. Guo J, Xu B, Han Q, Zhou H, Xia Y, Gong C, et al. Ferroptosis: a novel anti-tumor action for cisplatin. Cancer Res Treat 2018;50:445–60.
49. Magtanong L, Ko PJ, To M, Cao JY, Forcina GC, Tarangelo A, et al. Exogenous monounsaturated fatty acids promote a ferroptosis-resistant cell state. Cell Chem Biol 2019;26:420–432.e9.